Core-level and valence band photoemission study of $La_{1-x}Sr_xMnO_3$ perovskite oxide powders synthesized by mechanically and thermally activated solid-state reaction

1999 J. Phys.: Condens. Matter 11 3387

(http://iopscience.iop.org/0953-8984/11/16/018)

J. Phys.: Condens. Matter **11** (1999) 3387–3393. Printed in the UK PII: S0953-8984(99)99945-9

Core-level and valence band photoemission study of $La_{1-x}Sr_xMnO_3$ perovskite oxide powders synthesized by mechanically and thermally activated solid-state reaction

A Santoni†, G Speranza‡, M R Mancini†, F Padella†, L Petrucci† and S Casadio†

† ENEA-INN, Divisione Nuovi Materiali, C R Casaccia, CP 2400, I-00100 Roma, Italy
‡ IRST-ITC, via Sommarive, I-38050 Povo, Italy

Received 7 December 1998, in final form 19 February 1999

Abstract. High-resolution core-level and valence band x-ray photoemission spectroscopy measurements were performed on $La_{1-x}Sr_xMnO_3$ perovskite oxide powders synthesized for applications in solid-oxide fuel cells by high-temperature solid-state reaction ($x = 0.3$ and 0.19) and by room-temperature mechanical activation of the precursors ($x = 0.3$). A structure in the valence band at about 1 eV below the Fermi level was clearly observed and assigned to the emission from the Mn 3d-derived $e_g^1\uparrow$ states, thereby allowing the extraction of information about correlation effects in this type of material. Both the core-level and valence band spectral features were found to be independent of the choice of synthesis route. This finding indicates that mechanical activation, due to its lower synthesis temperature, can represent a valid alternative method of synthesis allowing a better control of the microstructure.

1. Introduction

Mixed-valence manganese perovskite oxides, such as $La_{1-x}M_xMnO_3$ (M = Ca, Sr, ...), exhibit a variety of electrical, magnetic and catalytic properties which, apart from the developments based on the colossal magnetoresistance effect [1], also make them attractive for several electrochemical applications and especially as solid-oxide electrodes in high-temperature fuel cells [2].

$LaMnO_3$ contains Mn in the 3^+ oxidation state and the substitution at some La sites of alkaline-earth elements induces a partial oxidation of Mn^{3+} to Mn^{4+}, and the system becomes mixed valence. These perovskite oxides are known to be ferromagnetic conductors for doping concentrations ranging from about 0.2 to 0.4 while the end compounds ($x = 0$ or 1) are antiferromagnetic insulators [3]. The simultaneous occurrence of ferromagnetism and metallic behaviour is explained by a spin-dependent scattering mechanism (double exchange) and is associated with the presence of both Mn^{3+} and Mn^{4+} ions [4].

The conventional solid-state-reaction (SSR) method requires repeated mixing and extended heating at high temperature to generate a homogeneous and single-phase material. The side effects of this procedure are a limited control of the microstructure and a low specific area of the synthesized materials. These hinder the achievement of porous, low-grain-size and homogeneous-grain-distribution 'screen-printed' layers on zirconia substrates which are needed to obtain well performing electrocatalytic properties [5]. In order to overcome

0953-8984/99/163387+07$19.50

these drawbacks, alternative methods such as the sol–gel, co-precipitation and ball-milling techniques have been used, as is reported in the literature [6].

Low-temperature techniques, such as near-room-temperature ball milling, offer the possibility of forming structures with new properties [7]. In order to try to improve the cathode performance in solid-oxide fuel cells (SOFC), a new process based on near-room-temperature synthesis of nanocrystalline Sr-doped $LaMnO_3$ by high-energy ball milling was developed. By subsequent low-temperature heating (700 °C) the system could be promoted completely to high-purity Sr-doped $LaMnO_3$ [8].

In this paper we present a core and valence band x-ray photoemission spectroscopy (XPS) investigation of a $La_{0.7}Sr_{0.3}MnO_3$ powder synthesized by means of low-temperature mechanical activation. In addition, XPS data taken on mixed-valence Sr-doped $LaMnO_3$ synthesized by the traditional solid-state-reaction method are also presented for comparison.

2. Experimental procedure

Following the traditional SSR method, $La_{1-x}M_xMnO_3$ ($x = 0$, 0.19 and 0.3) powders were obtained by heating a mixture of La_2O_3, $SrCO_3$ and MnO_2 at 900 °C in air for 24 h, with intermediate grinding steps. The x-ray diffraction analysis showed the formation of a pure perovskite phase for the $x = 0$ and $x = 0.3$ concentrations, while in the $x = 0.19$ sample traces of $La(OH)_3$ were found. In order to obtain a material identical to that employed as a cathode for solid-oxide fuel cells, pellets of different densities (60% and 95% of the theoretical density) were prepared for each composition by sintering at 1200 °C and 1500 °C.

The mechanically activated process was carried out by milling the precursors in a high-energy ball-milling device (Fritsch Pulverisette 5). Two different mixtures of precursors consisting of (i) La_2O_3 and MnO_2 and (ii) La_2O_3, MnO_2 and $SrCO_3$ were employed to obtain the undoped and the Sr-doped ($x = 0.3$) La manganite systems respectively. The process was performed in air at 300 rpm with adequate cooling using stainless steel vials filled with 10 mm stainless steel balls. The powder-to-ball mass ratio was chosen to be 1:10. X-ray diffraction analysis showed that a La manganite phase began to nucleate in both systems after two hours of milling. After 25 hours of milling time, each system was found to consist of a nanocrystalline manganite phase coexisting with an amorphous phase. The amorphous phase is due to unreacted precursors which are highly destabilized by the milling action. For both samples the specific area was 25 ± 5 m^2 g^{-1}. Pure undoped and Sr-doped La manganite were obtained by heating the milled powders at 700 °C for six hours. Pellets were prepared by sintering at 1200 °C.

The photoemission measurements were performed at room temperature in an UHV system (base pressure $\simeq 5 \times 10^{-10}$ mbar) equipped with an angle-integrated Scienta 200 spectrometer and a monochromatized Al Kα x-ray source. The core-level spectra and the valence band (VB) data were taken at normal emission at total resolutions of 0.35 eV and 0.5 eV respectively, as determined from the Fermi edge of a clean Au sample. All of the binding energies are referred hereafter to the Fermi level. The sintered powder samples were cracked in vacuum in a preparation chamber and then transferred into the main chamber for analysis. No surface charging was observed in the semiconducting samples. The valence band and O 1s spectra taken at the beginning and at the end of the measurement cycles did not show any visible change, indicating negligible degradation effects.

3. Results and discussion

Figures 1(a) and 1(b) show the XPS O 1s spectra taken on samples synthesized by traditional solid-state reaction (SSR) with the Sr concentrations $x = 0.3$ (figure 1(a)) and $x = 0.19$ (figure 1(b)) and sintered at 1200 °C and 1500 °C. Figure 1(c) shows the O 1s XPS lineshapes measured for the mechanically activated (MA) sample. A linear background was subtracted from the spectra. In each panel the O 1s spectrum of the undoped $LaMnO_3$ is also shown for reference. The binding energy of the O 1s peaks in the SSR samples (figures 1(a) and 1(b)) is found at 529.2 ± 0.05 eV for both concentrations and temperatures. The O 1s binding energy in the MA sample (figure 1(c)) is found at 529.3 ± 0.05 eV. According to earlier results [9, 10], the O 1s peak energy positions for the undoped samples are at higher binding energy and they are found at 529.5 ± 0.05 eV for the SSR samples and at 529.6 ± 0.05 for the mechanically activated one. In the case of the SSR samples, the intensity of the shoulder on the higher-binding-energy side of the O 1s spectra which is usually associated with contaminants on the surface [10] is observed to decrease as a function of increasing sintering temperature. The analysis of the C 1s spectra showed that the intensity of the shoulder is not correlated with the amount of C on the surface. On the other hand, O 1s peak fitting showed that the spectral intensity around 531.5 eV could be linked to the amount of Sr in the sample. In the SSR

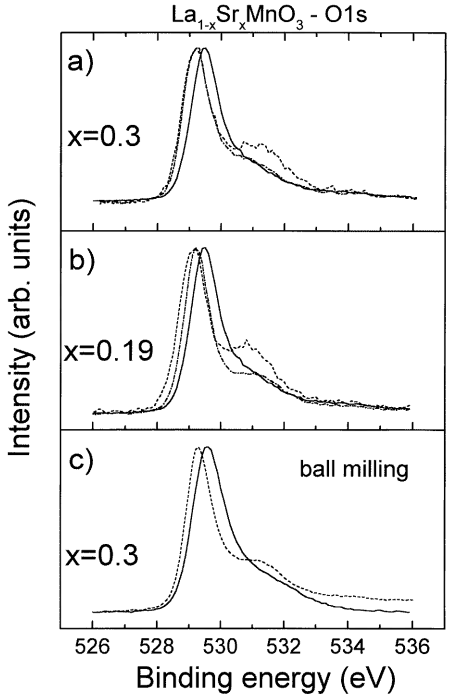

Figure 1. O 1s core-level XPS spectra taken with monochromatic Al Kα radiation at a total resolution of 0.35 eV. In each of the panels, (a), (b) and (c), the O 1s reference spectrum of the undoped $LaMnO_3$ is drawn as a continuous curve. (a) O 1s spectra of the SSR $La_{1-x}Sr_xMnO_3$ samples for $x = 0.3$ and the sintering temperatures 1200 °C (dashed curve) and 1500 °C (dotted–dashed curve). (b) O 1s spectra of the SSR $La_{1-x}Sr_xMnO_3$ samples for $x = 0.19$ and the sintering temperatures 1200 °C (dashed curve) and 1500 °C (dotted–dashed curve). (c) The O 1s spectrum of the ball-milling mechanically activated $La_{1-x}Sr_xMnO_3$ sample for $x = 0.3$ (dashed curve).

samples, the full width at half-maximum (FWHM) of the O 1s main peaks for the $x = 0.3$ samples is 1.1 ± 0.04 eV for both temperatures, and the same FWHM value is also found for the undoped sample. For $x = 0.19$ we found an O 1s FWHM value of 1.1 ± 0.04 eV for the 1200 °C sample and a value of 0.96 ± 0.04 eV for the 1500 °C sample. The spectral shape of the O 1s peak of the sample sintered at 1500 °C shows a loss of intensity on the lower-binding-energy side (see figure 1(b)). This is probably due to a lower emission from contamination-related components.

The O 1s FWHM value of the Sr-doped ($x = 0.3$) mechanically activated sample is 1.1 ± 0.04 eV. On the other hand, the FWHM of the O 1s peak for the undoped reference (the continuous curve in figure 1(c)) turns out to be 1.4 ± 0.04 eV. Excluding sample charging and considering that the XRD spectra of both the undoped MA and SSR sintered samples did not show any significant difference, we believe that this broadening is due to the presence of extra contamination-related O 1s components.

The XPS measurements were also performed on other significant photoemission lines such as La 3d, Mn 2p, Mn 3s and Sr 3d. The La $3d_{3/2}$ and $3d_{5/2}$ spin–orbit components are each split into a doublet structure corresponding to states with the configurations $\underline{3d}^9 4f^0 L$ and $\underline{3d}^9 4f^1 \underline{L}$ where L indicates the oxygen ligand and the underlining denotes a hole. The energy separation of the doublet structure measured on the La $3d_{5/2}$ component was found to be, for all of the samples, 4.3 ± 0.1 eV. Like for previous results on Ca-doped cobaltites [9], hole doping is found to shift the La 3d photoemission peak to lower binding energy. In our Sr-doped manganite systems, the shift was measured to be 0.3 ± 0.1 eV. The shift has the same magnitude and direction as that observed for the O 1s peak and, within the experimental accuracy, did not show any dependence on the method of synthesis, the concentrations ($x = 0$, 0.19 and 0.3) or the sintering temperatures (1200 °C and 1500 °C). According to previous results [10], the shift is to be interpreted as a change of the chemical potential. Within the experimental accuracy, the energy position of the Mn 2p lines was found to be constant. The exchange splitting exhibited by the Mn 3s core-level photoemission line [10] was found to be dependent on the doping. In agreement with the results reported by Saitoh *et al* in reference [10], the magnitude of the splitting was found to decrease on increasing x and measured to be 5.3 ± 0.3 eV for $x = 0$ and 4.7 ± 0.3 eV for $x = 0.3$. This indicates that the extra holes (of mainly p character) injected into $LaMnO_3$ are antiferromagnetically coupled to the high-spin d^4 configuration of the Mn^{3+} ions. For all of the samples on which measurements were made, the binding energy positions, the measured shifts and the splittings discussed above are summarized in table 1.

Table 1. The XPS binding energies in eV (referred to the Fermi level) of the La $3d_{5/2}$, Sr $3d_{5/2}$ and Mn $2p_{3/2}$ core levels of the samples synthesized by solid-state reaction (SSR) and by mechanical activation (MA), discussed in the text. The exchange-splitting values (ΔS: Mn 3s) extracted from the Mn 3s spectra and the splitting values (ΔS: La 3d) extracted from the La $3d_{5/2}$ spectra are also shown.

	La $3d_{5/2}$ (eV)	ΔS: La 3d (eV)	ΔS: Mn 3s (eV)	Sr 3d (eV)	O 1s (eV)	Mn $2p_{3/2}$ (eV)
SSR undoped	834.0 ± 0.1	4.3 ± 0.1	5.3 ± 0.3		529.5 ± 0.1	641.3 ± 0.3
$x = 0.3$, 1200 °C	833.7 ± 0.1	4.2 ± 0.1	4.8 ± 0.3	132.3 ± 0.1	529.2 ± 0.1	641.5 ± 0.1
$x = 0.3$, 1500 °C	833.6 ± 0.1	4.3 ± 0.1		132.4 ± 0.1	529.2 ± 0.1	641.5 ± 0.1
$x = 0.19$, 1200 °C	833.8 ± 0.1	4.2 ± 0.1	4.9 ± 0.3	132.5 ± 0.1	529.2 ± 0.1	641.7 ± 0.1
$x = 0.19$, 1500 °C	833.8 ± 0.1	4.3 ± 0.1		132.6 ± 0.1	529.2 ± 0.1	641.5 ± 0.1
MA undoped	834.2 ± 0.1	4.4 ± 0.1	5.5 ± 0.3		529.6 ± 0.1	641.3 ± 0.3
MA $x = 0.3$	833.9 ± 0.1	4.3 ± 0.1	4.8 ± 0.3	132.6 ± 0.1	529.3 ± 0.1	641.2 ± 0.3

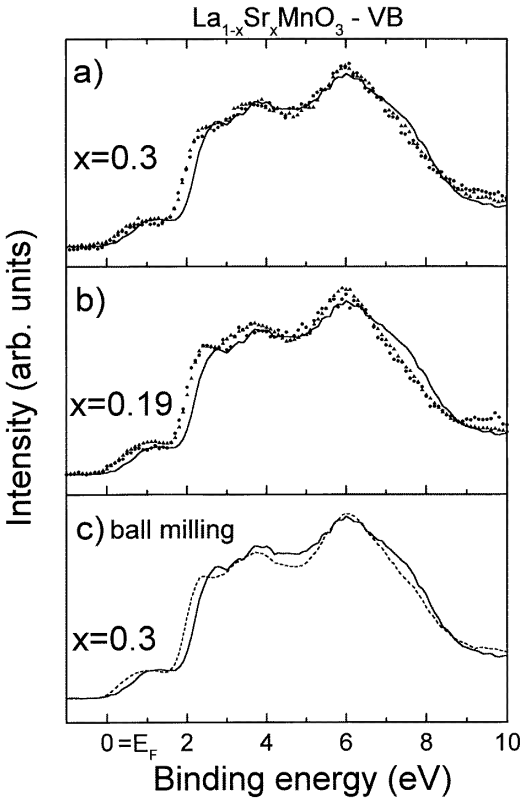

Figure 2. Valence band XPS spectra taken with monochromatic Al Kα radiation at a total resolution of 0.5 eV. In each of the panels, (a), (b) and (c), the valence band spectrum of the undoped $LaMnO_3$ reference is drawn as a continuous curve. (a) Valence band spectra of the SSR $La_{1-x}Sr_xMnO_3$ samples for $x = 0.3$ and the sintering temperatures 1200 °C (dots) and 1500 °C (triangles). (b) Valence band spectra of the SSR $La_{1-x}Sr_xMnO_3$ samples for $x = 0.19$ and the sintering temperatures 1200 °C (dots) and 1500 °C (triangles). (c) The valence band spectrum of the ball-milling mechanically activated $La_{1-x}Sr_xMnO_3$ sample for $x = 0.3$ (dashed curve).

Figures 2(a) and 2(b) show the XPS valence band (VB) spectra measured on the sample grown by SSR with concentrations $x = 0.3$ and $x = 0.19$ respectively and sintered at different temperatures. Figure 2(c) shows the XPS VB spectra obtained for the samples obtained by mechanical activation. A constant background was subtracted from all of the spectra before the normalization to the total area. In each panel the VB of the undoped sample is also shown for reference (continuous curve). For each sample, the VB data show a shoulder at about 1 eV, another shoulder at 2.4–2.7 eV and two further peaks at 3.6 eV and 6 eV. The overall shape of the VB is in good agreement with previously reported XPS data obtained by Chainani *et al* [11]. Due to the improved experimental resolution, our XPS data show a structure at about 1 eV below E_F which was not clearly observed in previous XPS studies [12]. In reference [10], Saitoh *et al* considered the featureless region of about 1–1.5 eV below E_F in their UPS data as due to the emission of the Mn 3d $e_g^1\uparrow$ band. In recent work by Suga *et al* [13], Mn 3d-derived valence band features were observed at 7 eV, 2.5 eV and just below the Fermi level E_F for $Nd_{0.5}Sr_{0.5}MnO_3$ by high-resolution resonant photoemission.

Theoretical local spin-density approximation (LDA) and LDA + U [14, 15] studies show

an appreciable density of states (DOS) at about 1 eV for $LaMnO_3$. In particular, the work by Satpathy *et al* [14] shows a LDA DOS due to emission from the Mn $e_g^1\uparrow$ band at about 1 eV and emission from the Mn $t_{2g}\uparrow$ band at about 2 eV below E_F. According to their LDA + U_2 model, where only t_{2g} electrons are considered as localized whereas the e_g ones are treated as itinerant, Solovyev *et al* [15] predicted similar structures for the valence band of $LaMnO_3$. It is worth noting that in reference [14] the partial DOS shows that the oxygen contribution in the region just below the Fermi edge is very low. This would explain the results of UPS He I [11] and He II [10] measurements which, despite the favourable cross-section for O, recorded a low emission in the region of about 1 eV below E_F. The LSDA band structure calculated in reference [14] agrees with optical transmission data [17, 18] which found a $t_{2g}\uparrow$–$e_g^1\uparrow$ band separation of about 1.5 eV and the O_{2p} band located at ∼3 eV from E_F. Additional recent resonant photoemission work by Kuwata *et al* [19] assigned a structure at 2.5 eV to the Mn 3d $t_{2g}\uparrow$ states.

On the basis of the consideration explained above, we assign the observed feature at about 1 eV to the emission from the Mn 3d $e_g^1\uparrow$ band and the features at about 2.7 eV (for $x = 0$) and at about 2.4 eV (for $x = 0.19$ and 0.3) in the $La_{1-x}Sr_xMnO_3$ VB spectrum as mainly due to the emission from the Mn 3d $t_{2g}\uparrow$ band. The structures at ∼3.6 eV and 6 eV reflect O 2p states.

The experimental identification of the Mn $e_g^1\uparrow$ band at about 1 eV binding energy sheds new light on the role of electron correlations in Mn-type perovskite oxides and indicates that the $LaMnO_3$ band structure is characterized by a parameter representing a minimum effective Coulomb interaction for the t_{2g} states, and hence it can be successfully explained within the framework of the LSDA approach [15, 16].

The different synthesis methods seem not to influence the shape of the VB. Similarly, the SSR VB spectra turn out to be unaffected by the different concentrations and sintering temperatures applied to the samples. On the other hand, for all samples the injection of holes (see figures 2(a) and 2(b)) causes a shift of about 0.3 eV towards the Fermi level of the features found in the $x = 0$ VB spectrum at ∼2.7 eV and ∼1 eV. The magnitude of the shift is the same for both Sr concentrations. This effect has also been reported by Saitoh *et al* in reference [10], who observed in their He II UPS spectra a shift of about 0.4 eV on going from $x = 0$ to $x = 0.3$. Like for the core-level cases explained above, this shift can also be interpreted as a change of the chemical potential. The intensity of the feature at ∼1 eV compared with that of the undoped sample (continuous curves in figures 2(a), 2(b) and 2(c)) does not show any visible changes, within the statistics, as a function of increasing doping.

In conclusion, we have performed a high-resolution XPS study of the electronic structure of Sr-doped $LaMnO_3$ obtained by solid-state reaction and by mechanical activation. The core-level spectral features were found to be in agreement with the data reported in the literature and indicated that from the point of view of the electronic structure the two different synthesis methods produce equivalent materials. The same conclusion can be extracted from the analysis of the valence bands which also showed similar behaviours for all of the materials investigated. It turns out that, compared with the traditional SSR method, mechanical activation has the important advantage that it requires a lower temperature for synthesizing the manganite, thereby allowing a better control of the microstructure. It is worth noting that the VB data show that different contamination levels, as qualitatively determined from the O 1s spectra, induce no appreciable changes in the measured valence bands. Features at about 1 eV and 2 eV below the Fermi level could be observed and were assigned to emission from Mn 3d $e_g^1\uparrow$ and $t_{2g}\uparrow$ states respectively. The observation of the Mn 3d $e_g^1\uparrow$ band at 1 eV binding energy shows that $LaMnO_3$ band structure is characterized by a parameter representing a minimum effective Coulomb interaction for t_{2g} states.

Acknowledgments

We would like to thank Drs E Incocciati, F Cardellini and V Contini for their helpful contribution to the measurements.

References

[1] Kusters R M, Singleton J, Keen D A, McGreevy R and Hayes W 1989 *Physica* B **155** 362
Chabara K, Ohno T, Kasai M and Kozono Y 1993 *Appl. Phys. Lett.* **63** 1990
von Helmolt R, Wecker J, Holzapfel B, Schultz L and Samwer K 1993 *Phys. Rev. Lett.* **71** 2331
Jin S, Tiefel T H, McCormack M, Fastnacht R A, Ramesh R and Chen L H 1994 *Science* **264** 413
[2] Hammouche A, Siebert E and Hammou A 1989 *Mater. Res. Bull.* **24** 369
Minh N Q 1993 *J. Am. Chem. Soc.* **76** 563
Two J and Gallagher P K 1993 *Properties and Applications of Perovskite-Type Oxides* ed L G Tejuca and J L G Fierro (New York: Dekker)
[3] Jonker G H and Van Santen J H 1950 *Physica* **16** 337
Van Santen J H and Jonker G H 1950 *Physica* **16** 599
[4] Zener C 1951 *Phys. Rev.* **82** 403
Anderson P W and Hasegawa H 1955 *Phys. Rev.* **100** 675
de Gennes P G 1960 *Phys. Rev.* **118** 141
[5] Beie H J, Blum L, Drenckhahn W, Greiner H and Schichl H 1998 *3rd European Solid Oxide Fuel Cell Forum Proc. (Nantes)* ed P Stevens
[6] Baythoun M S G and Sale F R 1982 *J. Mater. Sci.* **17** 2757
Hashimoto T, Ishizawa N, Mizutani N and Kato M 1988 *J. Mater. Sci.* **2** 1102
[7] Froes F H, Russel K and Li C G 1994 *Int. J. Mechanochem. Mech. Alloy.* **1** 112
[8] Padella F, Incocciati E, Nannetti C A, Colella C, Casadio S and Magini M 1998 *Mater. Sci. Forum* **269–272** 105
[9] Vasquez R P 1996 *Phys. Rev.* B **54** 14 938
[10] Saitoh T, Bocquet A E, Mizokawa T, Namatame H, Fujimori A, Abbate M, Takeda Y and Takano M 1995 *Phys. Rev.* B **51** 13 942
[11] Chainani A, Mathew M and Sarma D D 1993 *Phys. Rev.* B **47** 15 397
[12] See for example the spectrum at $x = 0.3$ in figure 1 of reference [11].
[13] Suga S, Matsushita T, Tsunekawa M, Iwasaki T, Samejima J, Kuwata Y, Kimura A, Sekiyama A, Fujimori A, Ishii H, Miyahara T, Kuwahara H and Tokura Y 1997 *Physica* B **237+238** 413
[14] Satpathy S, Popovic Z S and Vukajlovic F R 1996 *Phys. Rev. Lett.* **76** 960
[15] Solovyev I, Hamada N and Terakura K 1996 *Phys. Rev.* B **53** 7158
[16] Sarma D D, Shanthi N, Barman S R, Hamada N, Sawada H and Terakura K 1995 *Phys. Rev. Lett.* **75** 1126
[17] Lawler J F, Lunney J G and Coey J M D 1994 *Appl. Phys. Lett.* **65** 3017
[18] Coey J M D, Viret M and Ranno L 1995 *Phys. Rev. Lett.* **75** 3910
[19] Kuwata Y, Suga S, Imada S, Sekiyama A, Ueda S, Iwasaki T, Harada H, Muro T, Fukawa T, Ashida K, Yoshioka H, Terauchi T, Sameshima J, Kuwahara H, Moritomo Y and Tokura T 1998 *J. Electron Spectrosc. Relat. Phenom.* **88–91** 281